Analytica Chimica Acta 1376 (2025) 344621

Contents lists available at ScienceDirect

Analytica Chimica Acta

journal homepage: www.elsevier.com/locate/aca

Quantification of heterocyclic aromatic compounds (NSO-HET) in fuels by offline HPLC-GC×GC-ToFMS

Pedro Victor Bomfim Bahia [a,b], Anaïs Rodrigues [c], Aleksandra Gorska [d], Paula Albendea [d], Djulia Bensaada [c], Pierre-Hugues Stefanuto [c], Jean-François Focant [c], Giorgia Purcaro [d], Maria Elisabete Machado [a,b,*]

[a] Universidade Federal da Bahia, Instituto de Química, Programa de Pós-Graduação em Química, 40170-115, Salvador, BA, Brazil
[b] Instituto Nacional de Ciência e Tecnologia em Energia e Ambiente - INCT E&A, Universidade Federal da Bahia, 40170-115, Salvador, BA, Brazil
[c] Organic and Biological Analytical Chemistry Group, MolSys Research Unit, University of Liège, 4000, Liège, Belgium
[d] Analytical Chemistry Lab, Gembloux Agro-Bio Tech, University of Liège, Gembloux, 5030, Belgium

HIGHLIGHTS

- NSO-HET quantification in fuels using unfractionated and fractionated samples.
- HPLC + GC × GC-ToFMS enables simultaneous quantification of 55 NSO-HET.
- First validated method for simultaneous NSO-HET analysis in fuels.
- Method suitable for routine analysis of a large number of samples.

GRAPHICAL ABSTRACT

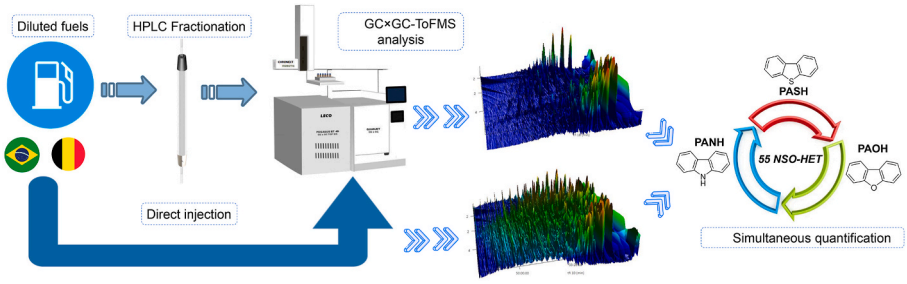

ARTICLE INFO

Keywords:
Nitrogen
Sulfur and oxygen compounds
Diesel and gasoline
Fuel
Comprehensive two-dimensional gas chromatography
Quantification

ABSTRACT

Background: Polycyclic aromatic heterocycles containing nitrogen, sulfur and oxygen (NSO-HET) are toxic and persistent contaminants commonly found in fuels. The simultaneous determination of NSO-HET is hindered by matrix complexity, isomer overlap, and coelution with aromatic compounds. Conventional approaches rely on laborious steps like fractionation to reduce the complexity of the matrix before chromatographic analysis. The resolution power of the comprehensive two-dimensional gas chromatography coupled with time-of-flight mass spectrometric (GC × GC-ToFMS) allows fewer sample preparation steps; however, quantification studies by this technique are limited. This study addressed the analytical challenge of simultaneously quantifying NSO-HET in complex fuels by GC × GC-ToFMS with minimal sample preparation.

Results: An offline preparative high-performance liquid chromatography (HPLC) method was applied to enrich the aromatic fraction and remove interferences, followed by GC × GC-ToFMS analysis of 55 NSO-HET across six fuel samples. Sample preparation was simplified, resulting in a reduction of solvent and sample manipulation. The method was validated and demonstrated adequate performance, with low limits of detection and quantification (0.34–70.34 ng mL^{-1}), recoveries from 56.6 % to 103 % and RSD values below 20 %. The method was successfully applied to both unfractionated and fractionated fuels. Marine diesel and diesel S-500 showed the highest concentrations, with 2,5,7-trimethylbenzothiophene and dibenzofuran at 943 ± 85.7 ng mL^{-1} and 884

* Corresponding author. Universidade Federal da Bahia, Instituto de Química, Programa de Pós-Graduação em Química, 40170-115, Salvador, BA, Brazil.
E-mail address: maria.elisabete@ufba.br (M.E. Machado).

https://doi.org/10.1016/j.aca.2025.344621
Received 18 July 2025; Received in revised form 4 September 2025; Accepted 5 September 2025
Available online 9 September 2025

± 31.7 ng mL^{-1}, respectively. Principal component analysis revealed significant discrimination among the samples based on compound class and concentration. This is the first study on the simultaneous quantification of a wide range of NSO-HET compounds in fuels samples by GC × GC-ToFMS.

Significance: The offline HPLC-GC × GC-ToFMS validated method enabled the accurate and simultaneous quantification of 55 individual NSO-HETs, including benzothiophenes, dibenzothiophenes, naphthobenzothiophenes, carbazoles, indoles, and dibenzofurans, in different fuels. It provides a robust alternative to traditional approaches for both industrial and research applications.

1. Introduction

Nitrogen, sulfur and oxygen compounds with the atom replacing a carbon in the aromatic ring comprise the heterocyclic aromatic class (NSO-HET) [1,2]. These compounds are commonly found in fuels and other petroleum refining products, even in low concentrations. This class can be subdivided into three different groups: polycyclic aromatic nitrogen heterocycles (PANH), polycyclic aromatic sulfur heterocycles (PASH) and polycyclic aromatic oxygen heterocycles (PAOH) [2]. The presence of PASH in fossil fuels can cause combustion problems that include catalyst poisoning and engine corrosion [1], as well as the release of these compounds into the environment, occasioning pollution and health issues, due to their recalcitrant and toxic characteristics [3,4]. Regarding PANH, its presence in diesel fuels can hinder the hydrodenitrogenation (HDN) and hydrodesulfurization (HDS) processes [5]. These hydrotreating steps are critical for removing nitrogen- and sulfur-containing species to meet fuel specifications, enhance stability, and limit NOx/SOx emissions; PANHs, particularly basic nitrogen heterocycles, adsorb strongly on the active sites of CoMo/NiMo catalysts, neutralize acid sites, and compete with sulfur compounds for hydrogenation/cleavage pathways, thereby lowering HDN/HDS conversion [5,6]. Meanwhile, PAOH have been found in petroleum and source rock samples, and some representatives of this class (e.g. benzofurans, dibenzofurans) are known to pose risks to human health and the environment [7].

The determination of NSO-HET in fuels is challenging. The complexity of the fuel sample, the relatively low concentrations of these analytes, and coelution between isomers and matrix interferents [2]. In this context, highly selective analytical methods are essential for effectively separating and identifying NSO-HET in these complex matrices.

The most commonly used sample preparation method for determining NSO-HET compounds in fuel samples is open-column liquid chromatography using SARA fractionation method (saturates, aromatics, resins and asphaltenes) [8–10]. However, it does not remove the matrix interference and neither solve all the coelution problems (e.g. PAHs and alkyl-PAHs), then an additional fractionation step of the aromatic portion is required [11,12]. There are two main selective fractionation systems for the obtaining PASH and PANH in petroleum or its derivatives, as palladium(II)-complex stationary phase [13,14] and silicic acid column and ion exchange chromatography, respectively [15,16]. The PAOHs are usually collected and analyzed in the aromatic fraction [17].

The sample preparation method for fuels requires large amounts of organic solvent and sample, and it is laborious, which can affect fractionation performance, leading to low recovery values. In this context, the use of high performance liquid chromatography (HPLC) in preparative mode as an alternative to replace the conventional method, since there will be a reduction in sample handling and the amounts of solvents used, it enables the reuse of the column for many analyses [18]. HPLC in preparative mode has already been applied to collect saturated and aromatic fractions analysis in various types of samples (e.g., food, petroleum products, environmental) prior to analysis [19–21].

The gas chromatography (GC) coupled to selective and specific detector techniques such as sulfur chemiluminescence detection (SCD) for PASHs [22], nitrogen chemiluminescence detector (NCD) for PANHs [23], or mass spectrometry (MS) [11,12,24] has been widely applied in fossil fuel sample analyses. Although GC-MS is a highly used technique, mainly due to the ability of MS to elucidate these compounds, its application in fuel analysis has some limitations. These include the incomplete compound separation and the number of isomers for NSO-HET, making simultaneous identification more difficult [2,14].

The comprehensive two-dimensional gas chromatography coupled to time-of-flight mass spectrometric detection (GC × GC-ToFMS) is a powerful analytical technique that presents greater peak capacity, resolution power, sensitivity and provides more detailed information when compared to the one-dimensional GC [25,26]. Furthermore, due to its higher ability to resolve interference from the analytes, the use of the technique allows the reduction of sample preparation steps. GC × GC-ToFMS has become a well-stablished and widely adopted technique in petroleum companies and analytical laboratories, where it is employed for the detailed characterization of complex hydrocarbon mixture [27]. It also has been successfully applied for the analysis of each PASH, PANH and PAOH class separately, in different types of fuels and petroleum products [3,13,14,28–33]. However, to the best of the authors' knowledge, there are no studies of the simultaneous determination of these three classes by GC × GC-ToFMS in fuel samples.

The aim of this study was to develop and validate an offline HPLC/GC × GC-ToFMS method for the simultaneous quantification of NSO-HETs in fuel samples.

2. Experimental

2.1. Reagents and standards

All detailed information about the NSO-HET standards is in the Supplementary Material (**Text S1**). The solvent dichloromethane (DCM, 99.9 %) was acquired from Merck (Darmstadt, Germany), isooctane (ISO, 99.5 %) was obtained from Sigma Aldrich (St. Louis, USA) and n-hexane (HEX, 99 %) for HPLC, previously distilled, was purchased from Biosolve Chemicals (Dieuze, France).

Stock solutions for each individual PASH, PANH and PAOH were prepared in isooctane at 10,000 ng mL^{-1}. Following, intermediate mix solutions (1000 ng mL^{-1}) were prepared for each class of compounds separately (20 PASHs + DBT-d_8; 18 PANHs + CA-d_8 and 9-PCA; 13 PAOHs + DBF-d_8) using the same solvent for the dilution process. A working standard solution was prepared by adding precise volumes of each intermediate mix solution at a concentration of 1000 ng mL^{-1}. Matrix-matched calibration curves were prepared using the aliphatic fraction mix prepared from each fuel, collected after fractionation on the HPLC (see Section 2.4.1), as matrix blank extract free of the analytes of interest, at eight concentration levels (n = 3) ranging from 10 to 1000 ng mL^{-1} (10, 25, 50, 100, 300, 600, 800 and 1000 ng mL^{-1}) for each compound.

2.2. Fuel samples

A total of six fuel samples was collected in gas station of two different places: four fuels are from Salvador, Bahia, Brazil: marine diesel (MD, ≤5000 ppm sulfur), diesel-S500 (D-S500, ≤500 ppm sulfur), diesel-S10 (D-S10, ≤10 ppm sulfur), gasoline (≤50 ppm sulfur) [34], and the other two fuels are from Gembloux, Belgium: diesel B7 (DB7, diesel with 7 % of biodiesel in the composition) and Euro 95 (E95, composed by 95 % of

octane and 5 % of heptane). The samples were adequately sampled in glass bottles, transported to the laboratory and stored at −20 °C until their analysis.

2.3. Sample preparation

Firstly, fuel samples were diluted 45-fold and 450-fold with n-hexane/DCM for subsequent direct injections. In order to evaluate the efficiency of the HPLC fractionation: 20 μL of each fuel sample was diluted 10-fold with *n*-hexane and after 10 μL of this solution was injected into the LC system (see parameters in Section 2.4.1). Then, 450 μL of the aliphatic and aromatic fractions were collected separately in fresh vials (45-fold dilution). Finally, the unfractionated samples and the aromatic fractions (45-fold and 450-fold) of each fuel were injected into GC × GC-ToFMS. Fig. 1 shows a schematic diagram of the sample preparation method.

2.4. Instrumentation and conditions

2.4.1. HPLC fractionation conditions

The fractionation of the fuel samples was carried out on an Agilent 1260 Infinity II LC equipped with an isocratic pump G7110B and a Variable Wavelength Detector (VWD) acquiring at 230 nm (Agilent Technologies, Waldbronn, Germany). The pump was modified by Axel-Semrau to ensure the minimization of the dead volumes. The HPLC was equipped with an Allure silica column (250 mm × 2.1 mm i.d. × 5 μm d_p) (Restek) and controlled by the software Clarity™ (DataApex, Prague, Czech Republic). The HPLC gradient program was as follows: 0 min 100 % n-hexane; 1.5–6.0 min reaches 35 % dichloromethane. Flow rate at 0.3 mL/min. After 6.10 min of the injection, the column was backflushed with dichloromethane at 0.5 mL/min for 9 min and then reconditioned at 0.5 mL/min with hexane for 10 min and at 0.3 mL/min for 5 min, until the following analysis [35].

The HPLC system was connected to a PAL3 Autosampler (PAL System from CTC, Switzerland) to perform the injections into the HPLC and the collection of fractions after LC separation in clean 2-mL vials. Then, the fractions obtained were analyzed using a Pegasus BT 4D GC × GC-FID (LECO Corp., St. Joseph, MI, USA). The HPLC method employed in this study was optimized in previous studies [35,36].

2.4.2. GC × GC-ToFMS univariate optimization

The NSO-HET analysis was carried out on a Pegasus BT 4D GC × GC-ToFMS (LECO, St. Joseph, MI, USA). Equipped with a secondary oven, a quad-jet dual-stage thermal cryo-free modulator (Peltier modulator) and a time-of-flight mass spectrometry (ToFMS). The first dimension (^{1}D) column was Rxi-5ms crossbond (5 % diphenyl/95 % dimethylpolysiloxane) (30 m × 0.25 mm × 0.25 μm); the second dimension column (^{2}D) was Rxi-17sil MS midpolarity crossbond phase (50 % diphenyl/50 % dimethylpolysiloxane) (2 m × 0.25 mm × 0.25 μm), this column set is the most employed for the determination of the NSO-HET [1,30,37,38]. The analytical GC columns were connected through a micro union (Trajan Scientific and Medical, USA). Given that the GC × GC method optimization entails substantial second- and third-order interactions among factors [39], a univariate (one-factor-at-a-time) strategy to tune individual parameters and maximize the analytical response was applied, according to prior studies [3,4,40]. Different conditions of the GC × GC were evaluated in order to obtain the best separation of the target analytes using a mix standard solution at 1000 ng mL^{-1}. A univariate optimization of the chromatographic method was performed and the following conditions were tested: injector temperature: 250 °C and 300 °C; temperature program: 1 °C min^{-1} and 3 °C min^{-1}; secondary oven temperature offset: +5 °C and +20 °C; period of modulation: 4, 6, and 8 s. The final program conditions optimized were: injector temperature: 250 °C, temperature program: 50 °C–310 °C (at 3 °C min^{-1}) with a difference between oven (ΔT) of 20 °C and modulation time: 4 s. Helium was used as carrier gas and the flow was set at 1.4 mL min^{-1} for the entire run. All samples were injected in liquid mode (1 μL). The injector was operated in split mode (split ratio of 1:10). Split ratios were needed to avoid overloading the detector signal. The ion source and the MS interface temperature were both operated at 250 °C. The acquisition rate was 200 spectra/s in the range of *m/z* 50−500. MS ionization mode: electron ionization (EI) at 70 eV. All the data acquisition and integration for the NSO-HET were performed using ChromaTOF™ software (LECO Corp., St. Joseph, MI, USA) version 5.56.53.

2.5. Validation of the analytical method

The methodology was validated according to the established by the International Union of Pure and Applied Chemistry (IUPAC) [41]: linearity of the range tested, LOD, LOQ, instrumental precision (intraday

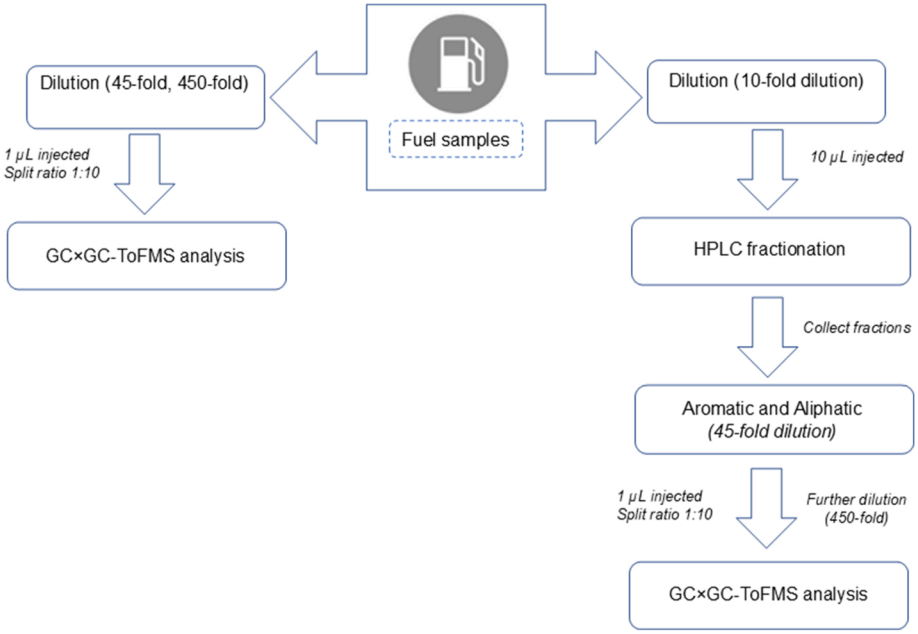

Fig. 1. Schematic diagram of the sample preparation method.

(n = 7) and interday (n = 21) tests), trueness, and selectivity.

The linearity was assessed by the correlation coefficient (R^2) obtained from the matched-matrix calibration curve and by analysis of the variance (ANOVA, $\rho < 0.05$) with a lack-of-fit test. The LODs and LOQs were determined from the calibration curve analysis by applying Eqs. (1) and (2): LOD = 3 SB/a (Eq. (1)) and LOQ = 10 SB/a (Eq. (2)), where "a" is the slope of the calibration curve and "SB" is the standard deviation of the linear coefficient. The precision intraday and interday were assessed as repeatability through the relative standard deviation (RSD, %) obtained from the injection of two standard solutions containing the 55 analytes (PASH, PANH and PAOH) at the concentrations of 100 and 600 ng mL^{-1}, respectively. For intraday tests, seven injections on the same day (n = 7) were executed. For the interday, seven injections were made on three different days (n = 21).

The method's trueness was assessed using addition/recovery tests at three different concentrations (100, 300 and 600 ng mL^{-1}). A mix of the aliphatic fractions (blank matrix) was spiked at each concentration in triplicate and subjected to the HPLC fractionation (as described in *Section 2.4.1*). The recoveries were expressed as the ratio (in %) between the concentration found after fractionation (aromatic fraction) of the enriched blank matrix and the known concentration added for each level of concentration. The selection of the concentration levels for the trueness and precision tests was made based on the possible concentration range in which NSO-HET are commonly found in fuel samples. To assess the selectivity, chromatograms of each aliphatic fraction and after enriching with 800 ng mL^{-1} of NSO-HETs were compared.

2.6. Statistical interpretation

For the interpretation of the data, the principal component analysis (PCA) was used in order to evaluate the relations and discriminate relevant information from the concentrations found for the NSO-HET in the unfractionated and fractionated fuels. The dataset was separated into three different matrices, one for each class of compounds, for the PASH (36 × 17), for the PANH (15 × 11), and for the PAOH (30 × 3), in which the samples are represented in rows and each PASH, PANH and PAOH concentrations are in the columns. For the initial pretreatment of the dataset, the concentration values were autoscaled to make them of equal significance. The criteria for extracting the principal components (PCs) was based on the screening test and eigenvalues ≥1 [42].

3. Results and discussion

3.1. Univariate optimization of the chromatographic method

The first chromatographic parameter evaluated was the injector temperature, with two values tested: 300 °C and 250 °C. In order to evaluate the behavior of the heaviest NSO-HETs, the highest injector temperature (300 °C) was applied in Test 1 (Fig. S1a and S1b), aiming to enhance the vaporization efficiency of these compounds. However, no significant difference was observed when compared to the results obtained at the lower injector temperature, as the heaviest compounds (e.g., B[b]CA, B[c]CA; Fig. S1b) were detected under both conditions. Therefore, the injector temperature was set at 250 °C for subsequent analyses.

Different temperature programs were also tested (**Test 2**, Fig. S2a and S2b; **Test 3**, Fig. S3a and S3b). At 3 °C min^{-1}, two coelution events were observed: (1) 2-MBF and 3-MBF and (2) 1-MDBF and 4-MDBF (*m/z* 131 and 182) (Fig. S2b). In order to solve this problem and obtain a good separation, another temperature program was tested, at 1 °C min^{-1}. However, no improvement was observed in the resolution of these coelution, and the analysis time almost doubled (161 min) (Fig. S3b). Therefore, the temperature program was set at 3 °C min^{-1}. The compounds involved in the coelution events were evaluated together as the sum of their concentration (2-;3-MBF and 1-;4-MDBF). Cases of coelution similar to those mentioned above have already been reported in the literature, such as between 2-MDBF and 3-MDBF [43]. In order to separate these analytes, more selective capillary columns would be required, such as cyanopropylphenyl, silicone stationary phase with specific geometry [16,44]. However, this semi-polar stationary phase also comes with limitations such as temperature limits and shorter lifetime.

The modulation period and the secondary oven temperature offset were the parameters that showed the greatest impact on the ^{2}D chromatograms and the results from these variations are reported in the Supplementary Material (Figs. S2a, S4a, S4b, S4c, S4d and S4e). Among the variations studied, 4 s of modulation and +20 °C for the secondary oven temperature offset (**Test** 2, Fig. S2a) were the conditions that presented the best result, since the reduction in modulation time and the temperature increase help to avoid wrapping around with aliphatic hydrocarbons or with alkyl-PAHs that are in high concentrations in the fuel samples [45].

Thus, the optimal chromatographic conditions for the determination of the NSO-HET analytes selected were: an injector temperature of 250 °C, an oven temperature program from 50 °C to 310 °C at 3 °C min^{-1} (total run time: 86.66 min), a secondary oven temperature offset of +20 °C relative to primary oven temperature, a modulation time of 4.0 s and a hot pulse duration of 1.20 s. A total ion chromatogram showing the optimal conditions of the GC × GC-ToFMS is given in Fig. 2 and in Table S2 are the retention times for the NSO-HETs.

3.2. Assessment of the LC fractionation

The aliphatic and aromatic fraction of each sample was collected and analyzed by GC × GC-FID, in order to evaluate the performance of the fractionation method. The information acquired was used to decide whether the obtained fraction was generally adequate to continue with subsequent analyses. Fig. S5 shows the total ion current (TIC) chromatograms of each fuel fraction obtained from the GC × GC-FID analyses. When comparing the chromatograms from the different fractions, in the regions marked for each class of compounds, it is possible to observe low or almost no presence of aliphatic compounds in the aromatic fraction and vice versa. Thus, the fractionation method applied was considered efficient for the samples tested regarding the separation of the aliphatic fraction from the fraction of interest.

3.3. Method validation

For method validation, matrix-matched calibration curves for the 55 NSO-HET exhibited correlation coefficients (R^2) values between 0.9912 (DBT-d_8) and 0.9975 (DBT) (Table 1). The test of lack-of-fit was applied to check the linearity of the calibration curve and all the ρ values obtained were >0.05, which indicates an adequate fit of the observed and predicted response values.

Values for LOD and LOQ were determined from the matrix-matched calibration curves, and the results varied between the compounds from different classes (Table 1). Toraman et al. (2016) [46] quantified PANHs compounds in bio-oil samples by GC × GC-ToFMS and reported LOD and LOQ values of 32.8 and 108.4 ng mL^{-1} for quinoline and 31.9 and 105.4 ng mL^{-1} for indole, respectively. Romanczyk et al. (2021) [5] quantified PANHs in petroleum-derived fuels using GC × GC-NCD, obtained LOD and LOQ for quinoline and carbazole ranges for 6.0 and 20.0 ng mL^{-1}. Notably, the LOD and LOQ reported in those studies were derived from calibration curves prepared in solvent and limited to a small number of analytes. In contrast, the values obtained in this study (Table 3) are significantly lower, underscoring the superior sensitivity of the proposed method.

For PASH, a greater sensitivity in this study was observed when comparing with results previously reported in the literature. For example, Aloisi and collaborators (2020) [29], determined eight organic sulfur compounds in coal tar samples by GC × GC-ToFMS and the LOD and LOQ values found for the compounds (BT, 2-MBT, DBT, 4,

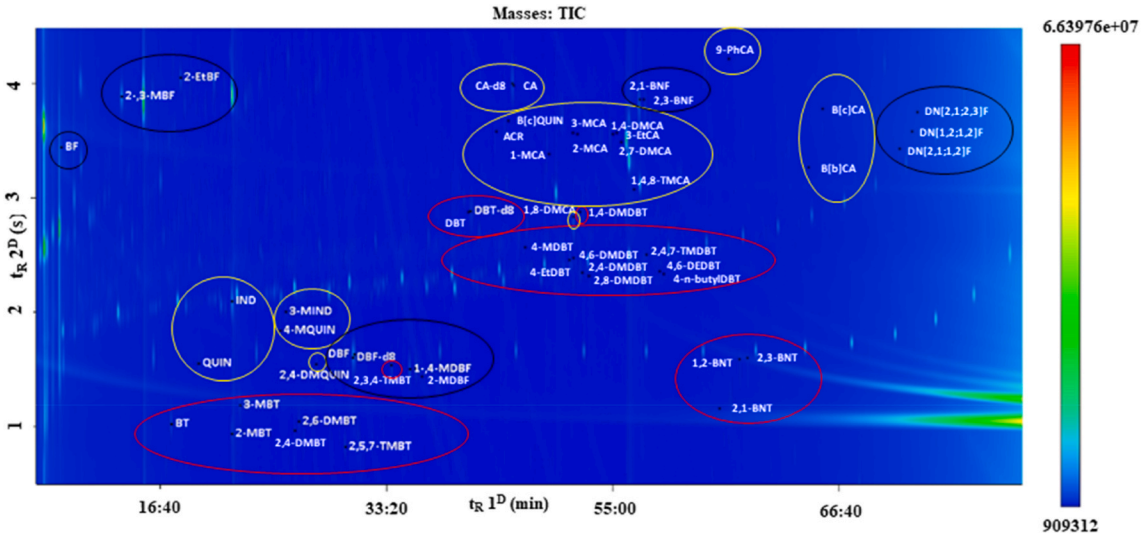

Fig. 2. Total ion current chromatogram resulting from the optimization of the chromatographic method for the NSO-HET (Red: PASH; Yellow: PANH; Black: PAOH). (For interpretation of the references to colour in this figure legend, the reader is referred to the Web version of this article.)

6-DMDBT) varied from 6000 to 10000 ng mL^{-1} and 20000–35000 ng mL^{-1}, respectively (Table 3). These values were about 524–9700 times higher than the LOD and LOQ found in this present study.

Specific LOD and LOQ values for PAOH analytes in complex matrices (e.g., crude oil, fuels, lubricating oil) using GC × GC-ToFMS as an analysis instrument are not widely reported in the literature, which makes it challenging to compare with the results obtained in this study.

The GC × GC-ToFMS instrumental precision tests were performed in two different concentrations (Table 1) and the results ranged from 4.9 to 12.6 % (intraday) and 6.4–18.0 % (interday) at 100 ng mL^{-1}, and 1.2–9.0 % (intraday) and 4.4–15.3 % (interday) at 600 ng mL^{-1}. These values did not exceed 20 % [41], confirming satisfactory precision for all compounds studied.

To assess the trueness of the method, addition/recovery tests were carried out in three different concentration levels (100, 300 and 600 ng mL^{-1}) and the results are presented in Table 2. The mean recovery values varied from 56.5 ± 1.7 to 78.5 ± 10.2 % (for 100 ng mL^{-1}), from 65.7 ± 8.3 to 95.4 ± 7.3 % (for 300 ng mL^{-1}) and from 60.3 ± 1.0 to 103 ± 1.0 % (for 600 ng mL^{-1}), with all the RSD <20 %. Recoveries for carbazole, its alkyl homologues and benzocarbazoles were not reported, since these analytes were retained in silica columns used for HPLC. DCM content up to 100 % was tested on silica column and these compounds (e.g., carbazole, benzocarbazoles) still did not elute in the aromatic fraction. Events of this nature have already been described by Dias et al. (2020) [9], who reported that silica gel columns are not suitable for the effective separation of nitrogen-containing compounds in crude oil samples. Silanol groups on the surface of silica gel can form hydrogen bonds and dipole-dipole interactions with carbazoles and benzocarbazoles (basic PANHs) through their pyrrolic NH, which leads to strong retention in the stationary phase and consequently influences their elution from silica columns [47]. The application of HPLC in preparative mode using C_{18} reverse-phase column already presented more suitable results in the separation of isomers of the C_1–C_4 carbazole classes in petroleum samples [48], which would be a more appropriate alternative specifically for PANHs class. There are other alternatives of HPLC columns with different stationary phases being used as an additional fractionation step after obtaining the aromatic fraction by open-column liquid chromatography, and they have shown an adequate response for the separation of PANH in crude oil and fuel samples, such as nitropropyl, silver, and aminocyan modified silica adsorbents [21,49,50]. No previous studies were found that evaluated the trueness of the method, using addition/recovery tests, by GC × GC-ToFMS analysis in fuels for a large number of compounds of the NSO-HET class.

The selectivity was evaluated after analysis of blank matrices (TIC chromatograms of each aliphatic fraction, Fig. S5) and the chromatogram of spiked blank aliphatic fraction at 800 ng mL^{-1} (Fig. S6). The interfering peaks from the aliphatic fraction mix components were present in the chromatogram at different retention times of the NSO-HET.

3.4. Application to unfractionated and fractionated fuel samples

The optimized and validated in GC × GC-ToFMS method was applied to six fuels, before and after HPLC fractionation (Table S2). For the PASH, seventeen out of twenty analytes were identified and quantified in the fractionated and unfractionated fuel samples. Fractionated marine diesel and S-500 showed the highest concentrations, ranging from 32.7 ± 3.3 (BT) to 943 ± 85.7 ng mL^{-1} (2,5,7-TMBT) and from 53.9 ± 8.7 (1,2-BNT) to 827 ± 59.0 ng mL^{-1} (4-EtDBT), respectively. For these samples, HPLC fractionation enhanced the identification and quantification of the PASH target compounds. For these samples, HPLC fractionation enhanced the identification and quantification of the PASH targets. This result is due to the removal of interfering compounds such as aliphatic and aromatic compounds, which dominate this kind of matrix. The fractionation reduces coelution events, leading to improved chromatographic resolution and sensitivity for PASH, as can be seen in Fig. 3 to the TIC and *m/z* 212, of class C_2-DBT, for non-fractionated and fractionated samples, respectively. For instance, the separation of compounds 2,4-DMDBT and 1,4-DMDBT from isomers and interferents would not be possible without the application of HPLC for the fractionation.

Gasoline is highlighted due to its considerable levels of light PASHs (BT to 2,3,4-TMBT), with concentrations ranging from 22.7 ± 1.8 (2-MBT) to 513 ± 5.7 ng mL^{-1} (2,4-DMBT), considering both unfractionated and fractionated samples. Contrarily, the S-10, D-B7, and Euro95, showed the lowest PASH levels, with only 5 compounds being determined, with concentrations ranging from 27.1 ± 0.04 (DBT) to 382 ± 77.6 ng mL^{-1} (4-EtDBT). All the PASH concentrations are shown in Fig. 4. 2,3,4-TMBT was the only PASH determined in all the fuel samples analyzed, which was aligned with the results found in Ref. [22], as 2,3,7-TMBT was one of the organic sulfur compounds with the highest content in military jet fuel samples analyzed by GC-MS-SCD [22].

Regarding the PANH class, only indole was evaluated in unfractionated and fractionated samples, whereas the rest of the PANH were evaluated only in unfractionated samples. PANH were found in all samples, except in Euro95 (Fig. 5a) and indole concentrations ranged

Table 1
Linear range, linearity, correlation coefficient (R^2), limits of detection (LOD), quantification (LOQ) and precision (RSD) of the method.

Compound	Linear range tested (ng mL^{-1})	Linearity		LOD (ng mL^{-1})	LOQ (ng mL^{-1})	Precision (100 ng mL^{-1}) (%)		Precision (600 ng mL^{-1}) (%)	
		(R^2)	Value ρ			Intraday (n = 7)	Interday (n = 21)	Intraday (n = 7)	Interday (n = 21)
PASH									
Benzothiophene	10.0–1000	0.9945	0.1484	4.30	14.33	8.2	14.7	1.6	6.3
2-methylbenzothiophene	10.0–1000	0.9943	0.1654	19.06	63.48	7.8	12.7	3.2	6.7
3-methylbenzothiophene	10.0–1000	0.9947	0.0869	10.47	34.86	8.4	11.6	2.3	5.9
2,4-dimethylbenzothiophene	10.0–1000	0.9961	0.6168	0.86	2.85	5.3	12.7	5.9	8.0
2,6-dimethylbenzothiophene	10.0–1000	0.9950	0.1710	7.00	23.33	12.6	15.0	2.8	5.3
2,5,7-trimethylbenzothiophene	10.0–1000	0.9947	0.1380	7.55	25.14	9.7	14.9	2.6	8.2
2,3,4-trimethylbenzothiophene	10.0–1000	0.9939	0.0819	10.29	34.28	10.5	11.7	2.5	12.4
Dibenzothiophene-d_8	10.0–1000	0.9912	0.4869	5.46	12.14	5.8	16.3	4.0	8.4
Dibenzothiophene	10.0–1000	0.9975	0.0693	0.92	3.06	8.4	16.6	2.1	6.4
4-methyldibenzothiophene	10.0–1000	0.9940	0.3266	5.34	17.79	7.4	15.3	5.0	12.4
4-ethyldibenzothiophene	10.0–1000	0.9943	0.056	9.33	31.07	6.0	12.1	6.0	10.9
4,6-dimethyldibenzothiophene	10.0–1000	0.9936	0.0697	1.54	5.13	5.8	18.0	4.8	13.7
2,4-dimethyldibenzothiophene	10.0–1000	0.9960	0.1344	1.04	3.47	6.4	13.6	1.2	11.1
2,8-dimethyldibenzothiophene	10.0–1000	0.9936	0.0576	2.63	8.75	9.3	9.7	8.5	15.3
1,4-dimethyldibenzothiophene	10.0–1000	0.9941	0.0516	1.08	3.62	5.5	8.3	2.5	9.3
2,4,7-trimethyldibenzothiophene	10.0–1000	0.9938	0.0519	1.60	5.34	5.1	10.9	6.7	9.2
4,6-diethyldibenzothiophene	10.0–1000	0.9933	0.5204	1.17	3.90	7.7	13.8	2.1	14.8
4-n-butildibenzothiophene	10.0–1000	0.9950	0.5623	5.28	17.58	7.9	14.7	2.2	8.2
Benzo[b]naphtho [2,1-d] thiophene	10.0–1000	0.9938	0.0519	1.77	5.90	7.1	15.3	3.7	7.3
Benzo[b]naphtho [1,2-d] thiophene	10.0–1000	0.9940	0.0517	1.44	4.78	9.3	12.9	8.3	10.8
Benzo[b]naphtho [2,3-d] thiophene	10.0–1000	0.9934	0.0514	1.57	5.22	5.4	6.8	2.8	10.9
PANH									
Quinoline	10.0–1000	0.9939	0.1302	2.07	6.91	6.0	13.2	3.3	8.6
Indole	10.0–1000	0.9935	0.0772	1.07	3.57	4.9	13.6	4.5	7.3
4-methylquinoline	10.0–1000	0.9934	0.3452	2.40	7.98	6.7	9.6	9.0	10.0
3-methylindole	10.0–1000	0.9944	0.1252	6.53	21.74	7.0	13.4	3.0	6.6
2,4-dimethylquinoline	10.0–1000	0.9939	0.0779	3.83	12.77	7.3	14.3	4.2	7.8
Acridine	10.0–1000	0.9935	0.3184	2.02	6.73	8.0	14.1	2.6	10.9
Benzo[c]quinoline	10.0–1000	0.9943	0.7613	3.25	10.84	5.9	12.6	7.6	11.2
Carbazole-d_8	10.0–1000	0.9950	0.0617	4.49	14.95	8.4	12.1	3.0	8.7
Carbazole	10.0–1000	0.9961	0.1363	0.80	2.67	9.6	14.5	3.2	14.3
1-methylcarbazole	10.0–1000	0.9940	0.2972	3.17	10.56	5.6	7.3	3.1	11.2
3-methylcarbazole	10.0–1000	0.9942	0.0768	0.95	3.17	4.5	6.4	4.7	8.8
2-methylcarbazole	10.0–1000	0.9937	0.6584	4.22	14.06	7.1	12.3	1.9	8.1
1,8-dimethylcarbazole	10.0–1000	0.9955	0.1005	4.52	15.06	7.1	11.1	6.5	10.9
1,4-dimethylcarbazole	10.0–1000	0.9942	0.3060	14.69	48.93	11.9	12.6	4.0	4.4
3-ethylcarbazole	10.0–1000	0.9932	0.0506	5.36	17.86	8.6	12.3	4.4	5.2
2,7-dimethylcarbazole	10.0–1000	0.9943	0.0514	6.85	22.82	10.9	12.3	2.1	3.7
1,4,8-trimethylcarbazole	10.0–1000	0.9943	0.1077	2.21	7.38	9.1	14.2	6.8	8.9
9-phenylcarbazole	10.0–1000	0.9929	0.1712	1.24	4.15	7.5	7.9	6.3	6.5
5-H-benzo[*b*]carbazole	10.0–1000	0.9950	0.2893	1.14	3.81	10.6	12.2	6.0	8.5
7-H-benzo[c]carbazole	10.0–1000	0.9939	0.8200	3.61	12.05	8.6	13.5	2.4	5.9
PAOH									
2,3-benzofuran	10.0–1000	0.9942	0.0552	16.86	56.17	8.7	10.5	6.5	8.2
2-methyl-/3-methylbenzofuran	10.0–1000	0.9944	0.1336	6.76	22.51	10.1	10.2	2.3	12.2
2-ethylbenzofuran	10.0–1000	0.9952	0.8847	2.95	9.84	7.0	13.2	2.0	3.9
Dibenzofuran-d_8	10.0–1000	0.9925	0.1248	21.12	70.34	5.0	11.1	4.9	7.9
Dibenzofuran	10.0–1000	0.9937	0.1473	0.34	1.14	6.6	9.0	4.3	8.3
1-methyl-/4-methyldibenzofuran	10.0–1000	0.9942	0.1423	0.63	2.08	8.5	16.3	8.4	6.9
2-methyldibenzofuran	10.0–1000	0.9936	0.7734	1.54	5.13	6.5	14.3	4.7	10.8
Benzo[b]naphtho[1,2-d]furan	10.0–1000	0.9937	0.0598	0.66	2.19	11.1	11.3	3.2	8.1
Benzo[b]naphtho[2,3-d]furan	10.0–1000	0.9934	0.0841	0.36	1.19	7.4	7.6	6.5	11.8
Dinaphto[2,1-b; 1,2-d]furan	10.0–1000	0.9932	0.4895	3.46	11.55	10.1	12.1	1.7	6.0
Dinaphto[1,2-b; 1,2-d]furan	10.0–1000	0.9935	0.3573	3.42	11.40	9.5	14.8	5.8	7.4
Dinaphto[2,1-b; 2,3-d]furan	10.0–1000	0.9948	0.6344	5.04	16.78	6.9	15.6	5.3	4.3

from 31.0 ± 0.22 to 693 ± 47.1 ng mL^{-1}. Fractionation in this case showed no significant differences in both concentration and identification. Similar to what was observed for the PASH class, marine diesel presented the highest concentrations, ranging from 169 ± 48.9 (2,7-DMCA) to 935 ± 191 ng mL^{-1} (1,8-DMCA), with 1,8-DMCA being the analyte with the highest content. Despite the few studies about PANH in fuels, Wang et al. (2004) [51] observed the C_2-carbazole class in considerable content (1380 ng mL^{-1}, Table 3) after GC × GC-NCD analysis, with this level being comparable with the ones found in this study for this class. For S-500, gasoline and S-10, the PANH levels were lower when compared to marine diesel and decreased in that order, varying from 30.3 ± 12.0 (1,4,8-TMCA, gasoline) to 295 ± 27.9 ng

Table 2
Mean recovery yields (±standard deviation, n = 3) in three concentration levels for accuracy assessment.

Compound	Added (100 ng mL^{-1})	Added (300 ng mL^{-1})	Added (600 ng mL^{-1})
PANH			
Quinoline	69.9 ± 7.1	71.8 ± 5.4	73.1 ± 4.4
Indole	59.6 ± 3.6	60.4 ± 1.2	61.2 ± 2.9
4-methylquinoline	n.d.	67.1 ± 0.8	71.7 ± 4.2
3-methylindole	62.6 ± 2.4	64.1 ± 7.7	64.7 ± 2.7
2,4-dimethylquinoline	61.2 ± 5.5	75.4 ± 2.5	78.6 ± 5.5
Acridine	60.8 ± 2.3	63.9 ± 3.5	68.2 ± 1.1
Benzo[c]quinoline	61.5 ± 6.2	70.5 ± 5.0	73.7 ± 2.1
Carbazole-d8	n.d.	n.d.	n.d.
Carbazole	n.d.	n.d.	n.d.
1-methylcarbazole	n.d.	n.d.	n.d.
3-methylcarbazole	n.d.	n.d.	n.d.
2-methylcarbazole	n.d.	n.d.	n.d.
1,8-dimethylcarbazole	n.d.	n.d.	n.d.
1,4-dimethylcarbazole	n.d.	n.d.	n.d.
3-ethylcarbazole	n.d.	n.d.	n.d.
2,7-dimethylcarbazole	n.d.	n.d.	n.d.
1,4,8-trimethylcarbazole	n.d.	n.d.	n.d.
9-phenylcarbazole	67.2 ± 0.7	73.5 ± 3.7	75.5 ± 0.5
5-H-benzo[*b*]carbazole	n.d.	n.d.	n.d.
7-H-benzo[c]carbazole	n.d.	n.d.	n.d.
PASH			
Benzothiophene	69.8 ± 1.1	75.5 ± 4.2	84.3 ± 1.4
2-methylbenzothiophene	69.9 ± 4.8	83.7 ± 0.4	90.0 ± 8.9
3-methylbenzothiophene	74.3 ± 4.8	77.7 ± 6.8	81.4 ± 8.2
2,4-dimethylbenzothiophene	69.5 ± 4.9	84.0 ± 2.6	87.7 ± 6.8
2,6-dimethylbenzothiophene	73.4 ± 1.9	81.8 ± 6.8	84.0 ± 2.6
2,5,7-trimethylbenzothiophene	71.9 ± 10.4	74.9 ± 3.8	79.5 ± 2.6
2,3,4-trimethylbenzothiophene	74.9 ± 3.0	78.8 ± 2.9	81.6 ± 2.5
Dibenzothiophene-d8	75.0 ± 6.2	83.1 ± 1.1	103 ± 1.0
Dibenzothiophene	78.5 ± 10.2	81.9 ± 2.3	82.5 ± 6.4
4-methyldibenzothiophene	78.1 ± 1.7	79.7 ± 3.9	79.9 ± 1.7
4-ethyldibenzothiophene	69.5 ± 8.0	72.7 ± 8.9	86.0 ± 7.7
4,6-dimethyldibenzothiophene	78.4 ± 1.8	79.2 ± 2.8	80.7 ± 8.2
2,4-dimethyldibenzothiophene	73.5 ± 6.4	77.2 ± 1.2	78.8 ± 0.5
2,8-dimethyldibenzothiophene	65.1 ± 2.7	76.0 ± 3.2	79.6 ± 1.2
1,4-dimethyldibenzothiophene	68.4 ± 1.8	72.3 ± 3.0	74.3 ± 5.1
2,4,7-trimethyldibenzothiophene	65.0 ± 1.5	69.7 ± 2.3	78.0 ± 9.9
4,6-diethyldibenzothiophene	63.3 ± 2.1	70.7 ± 7.1	76.8 ± 6.1
4-n-butildibenzothiophene	62.0 ± 4.5	68.8 ± 7.6	71.0 ± 3.3
Benzo[b]naphtho[2,1-d] thiophene	66.5 ± 4.3	74.7 ± 6.1	78.9 ± 2.9
Benzo[b]naphtho[1,2-d] thiophene	68.2 ± 3.8	75.2 ± 4.9	76.2 ± 4.2
Benzo[b]naphtho[2,3-d] thiophene	63.2 ± 1.1	69.9 ± 1.0	70.3 ± 4.5
PAOH			
2,3-benzofuran	67.2 ± 2.4	67.6 ± 5.9	70.7 ± 1.7
2-methyl-/3-methylbenzofuran	62.5 ± 3.1	73.6 ± 2.0	74.2 ± 1.9
2-ethylbenzofuran	66.6 ± 8.3	67.7 ± 1.5	68.2 ± 2.0
Dibenzofuran-d8	73.8 ± 0.8	74.1 ± 0.3	85.0 ± 0.5
Dibenzofuran	66.1 ± 4.8	69.8 ± 3.6	74.3 ± 5.3
1-methyl-/4-methyldibenzofuran	64.7 ± 7.0	69.6 ± 1.8	70.2 ± 1.8
2-methyldibenzofuran	68.4 ± 5.2	70.5 ± 2.2	83.2 ± 0.7
Benzo[b]naphtho[1,2-d]furan	63.4 ± 4.6	64.1 ± 0.7	70.5 ± 1.2
Benzo[b]naphtho[2,3-d]furan	60.7 ± 3.4	66.0 ± 5.6	75.5 ± 3.3
Dinaphto[2,1-*b*; 1,2-d]furan	62.2 ± 6.2	69.6 ± 4.3	69.7 ± 0.9
Dinaphto[1,2-*b*; 1,2-d]furan	60.5 ± 3.5	64.2 ± 2.1	65.7 ± 6.8
Dinaphto[2,1-*b*; 2,3-d]furan	56.5 ± 1.7	58.6 ± 5.7	60.3 ± 1.0

mL^{-1} (3-EtCA, D-S500). The PANH concentrations found in the fuel samples are shown in Fig. 5a.

DBF, 1-/4-MDBF and 2-MDBF were the PAOHs found in the fuel samples analyzed. Their concentrations ranged from 15.0 ± 0.1 (1-/4-MDBF; gasoline, fractionated) to 884 ± 31.7 ng mL^{-1} (DBF; diesel-S500, fractionated). Euro95 was the only sample in which no PAOHs were detected. The concentrations in both fractionated and unfractionated fuel samples for PAOHs are presented in Fig. 5b. DBF was the analyte found in the highest concentration in the samples (46.7 ± 9.3 gasoline, fractionated) to 884 ± 31.7 ng mL^{-1} (DBF; diesel- S500, fractionated). For PAOH, no considerable differences were observed when applying HPLC fractionation. To the best of our knowledge, this is the first study to quantify multiple PAOHs in fuels using GC × GC-ToFMS. Compounds such as dibenzofuran were reported in fuel samples [52–55], but employing GC-AED [52], GC × GC/HR-TOFMS [53], GC × GC-MS [54], or GC-MS [55]. In these studies, the sample preparation procedures were generally laborious, with fractionation in open-column chromatography followed by successive extraction steps prior to instrumental analysis. A comparison of the LOD, LOQ, and concentration values is shown in Table 3.

3.5. Statistical interpretation

PCA was employed for each NSO-HET class separately (PASH, PANH, PAOH), in order to evaluate the similarity and to discriminate relevant information from redundant data for the fractionated and unfractionated fuel samples. First, the loading and the score graphs were obtained from the PCA (36 × 17) for the PASH concentrations in the fuel samples (Fig. 6a and b). In total, two PCs were extracted, accounting for 74 % of the total variance (PC1 × PC2). For PC1, all the variables exhibited negative loadings contributing to the discrimination of the samples. The score plot (Fig. 6b) shows the formation of a large cluster containing D-S10, D-B7, gasoline, and Euro95 unfractionated and fractionated, separated from the fractionated and unfractionated marine diesel and D-S500 samples. This separation was due to the low concentrations of the analytes in later fuel samples, since this cluster was formed in the positive PC1.

In PC2, 4-EtDBT and BT showed high positive loadings (0.6458 and 0.4575) (Fig. 6a), as values ≥ 0.60 are considered significant for data interpretation [56]. 4-EtDBT was the analyte that contributed to the separation of the fractionated S-500 sample from the others. Meanwhile, 2,4,7-TMDBT was the PASH with the highest negative loading in this PC (−0.6668), leading to the separation of the unfractionated marine diesel sample from the rest (Fig. 6b), as 2,4,7-TMDBT was only found in this sample. 2,4,7-TMDBT has already been identified in crude oil samples by GC-MS [57]. However, studies have already reported that the third methyl group in this position (2,4,7-TMDBT) increases the molecule's reactivity [58], which facilitates its desulfurization. Marine diesel is the heaviest fraction of oil refining and contains the highest sulfur content among the fuel samples analyzed. As a result, it undergoes milder desulfurization processes, which may explain the presence of 2,4,7-TMDBT exclusively in this sample. Finally, PCA confirmed the significant impact of the HPLC fractionation for the determination of PASHs in marine diesel and S-500 samples.

Fig. 6 PCA was applied only to PANHs results from unfractionated fuel samples. PCA for the PANH (15 × 11) generated the loading graph (Fig. 7a), extracting two PCs that account for 96 % of the total variance of the data (PC1 × PC2). In PC1, all PANHs had negative loadings, distinguishing the samples D-S10, D-B7, and gasoline from the marine diesel and S-500 in the score graph (Fig. 7b), as they contained low or undetectable concentrations of the target analytes. On the other hand, in PC2, IND and CA had the highest positive loadings, aiding in differentiating the diesel S-500. The score graph (Fig. 7b) shows marine diesel and S-500 separated from the other samples in PC2. This differentiation was due to the presence of six PANHs (1-MCA, 3-MCA, 2-MCA, 2,7-DMCA, B[b]CA, and B[c]CA) only in the marine diesel sample and the

Table 3
Comparison of LOD, LOQ and concentration range results for NSO-HET using GC × GC in the literature.

Sample	Analytes	LOD/LOQ (ng mL^{-1})	Concentration range (ng mL^{-1})	Instrumentation	Ref.
Bio-oils	QUI and IND	QUI: 32.8/108.4; IND:31.9/105.4;	QUI: 0.16 ± 0.02; IND: 0.76 ± 0.01[a]	GC × GC-NCD	[46]
Petroleum derived	QUI and CA	6.0–20.0	–	GC × GC-NCD	[5]
Coal tar	BT, 2-MBT, DBT and 4,6-DMDBT	6000–10000/20000–35000	5.9×10^8–1.5×10^9	GC × GC-ToFMS	[29]
Diesel fuel	C_2-carbazole class	–	1380	GC × GC-NCD	[51]
	IND, ACR and CA	60–160	–	GC × GC-qMS	[56]
Bio-oils and petroleum derived	DBF	0.14–0.46[b]	0.006 ± 0.0002–0.028 ± 0.003[a]	GC × GC-MS	[54]

[a] The concentrations are expressed weight percent (wt%).
[b] LOD and LOQ are expressed in mg kg^{-1}.

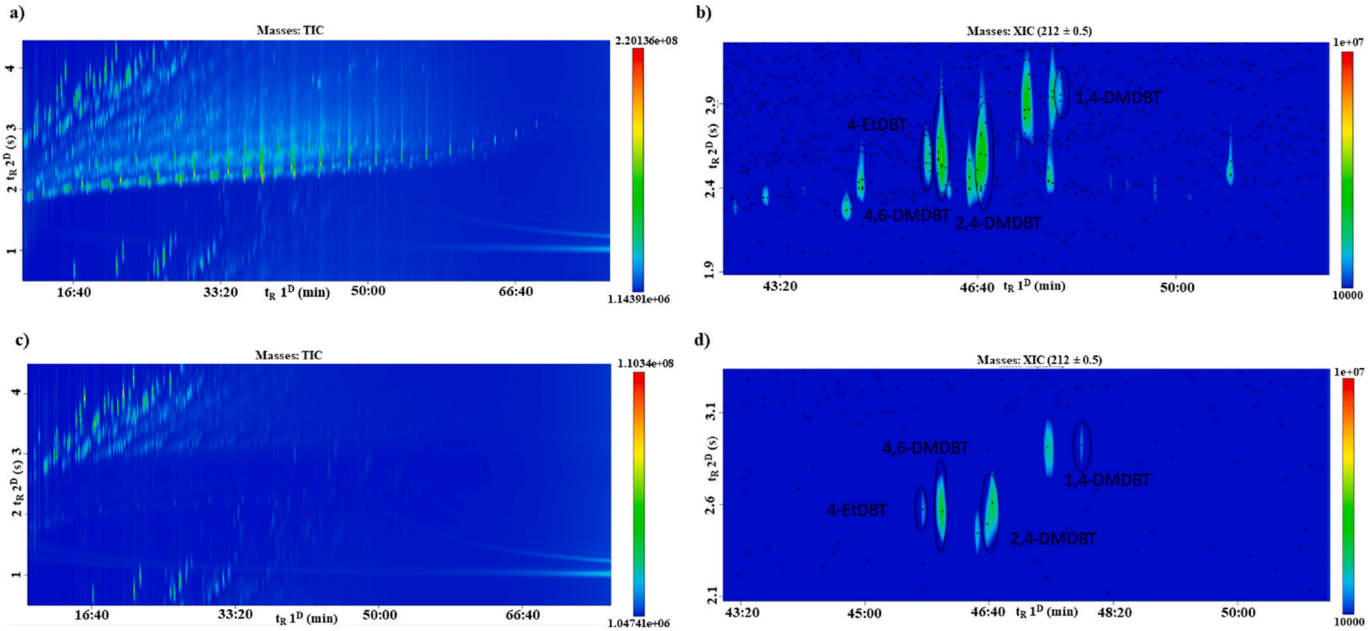

Fig. 3. Diluted marine diesel: **(a)** TIC and **(b)** the extracted ion (*m/z* 212). Aromatic fraction of marine diesel sample: **(c)** TIC and **(d)** the extracted ion (*m/z* 212).

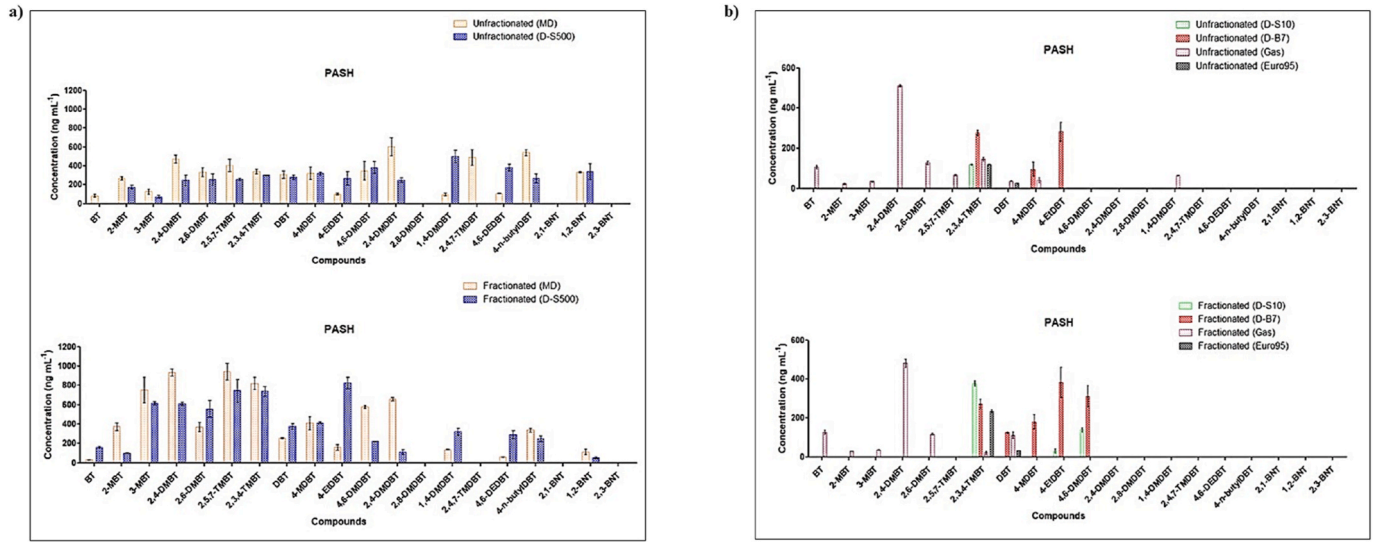

Fig. 4. Distribution of PASH concentrations in unfractionated and fractionated fuels: **(a)** marine diesel and diesel S-500, **(b)** diesel S-10, diesel B7, gasoline and Euro 95 samples (Concentration ± standard deviation).

high levels of IND in diesel S-500. Maciel et al. (2015) [59] monitored eight PANHs, including IND, in Brazilian diesel fuels by GC × GC-quadrupole mass spectrometry (qMS) and IND was detected in the diesel fuel analyzed without the need for pre-fractionation steps, which highlighted the power of resolution of the GC × GC (Table 3). Therefore, with the PCA result, it was possible to discriminate the fuel samples according to their nature, in which only the diesel samples S-10 and B7 appear grouped, due to the low levels of PANH.

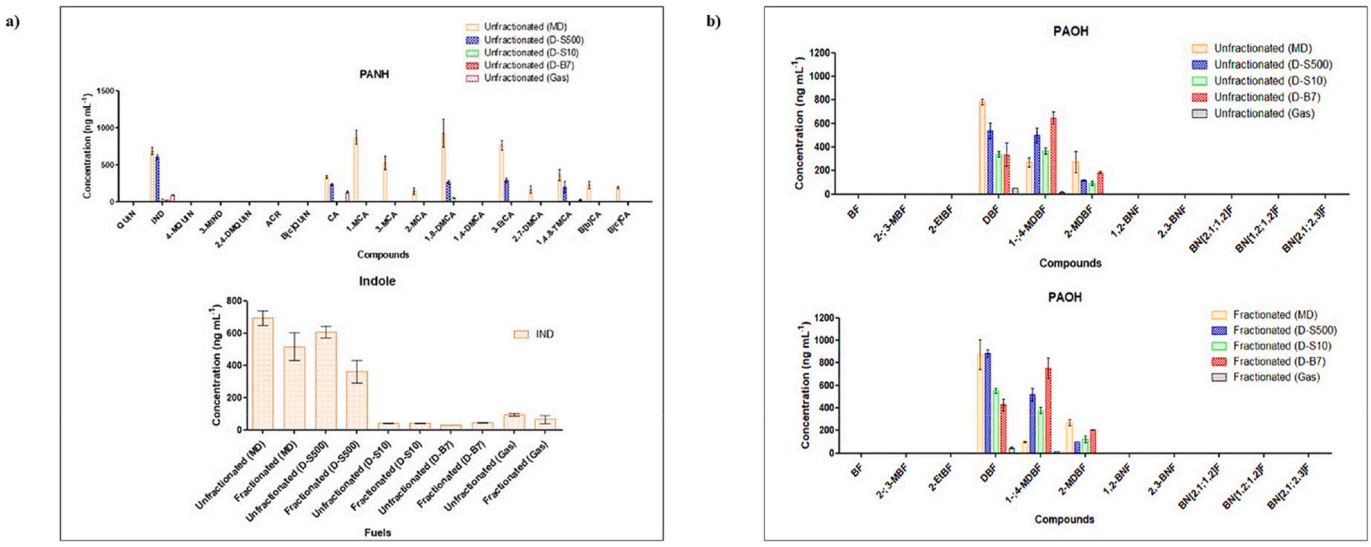

Fig. 5. Distribution of concentrations in unfractionated and fractionated fuels: **(a)** PANHs **(b)** PAOHs (Concentration ± standard deviation).

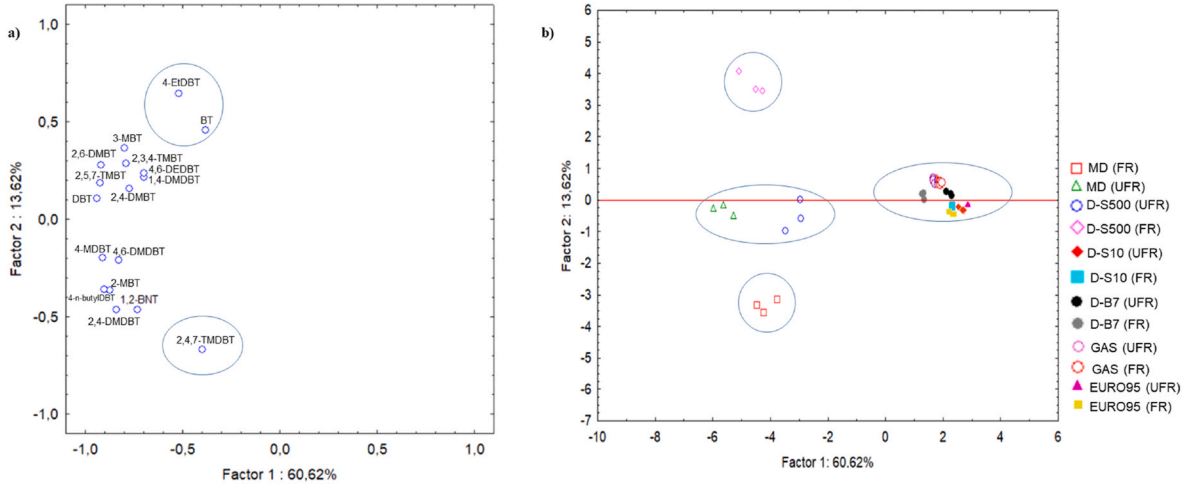

Fig. 6. Principal component analysis (PCA) for the PASHs found in unfractionated and fractionated fuel samples: **(a)** loading graph PC1 × PC2 and **(b)** score plot PC1 × PC2.

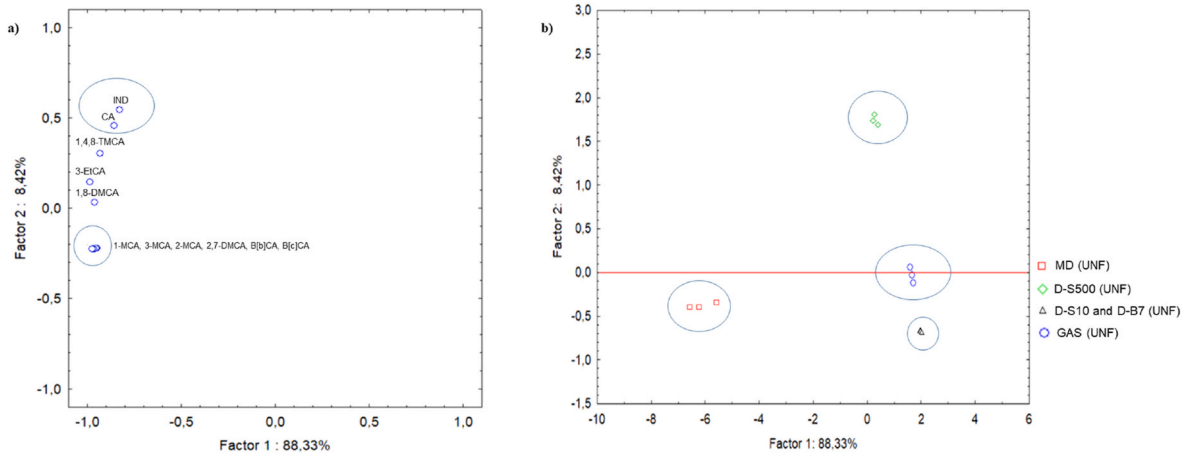

Fig. 7. PCA for the PANHs found in unfractionated fuel samples: **(a)** loading graph PC1 × PC2 and **(b)** score plot PC1 × PC2.

Regarding PAOHs, PCA (30 × 3) was generated and provided loading and score graphs (Fig. S7a and b). Despite extracting two PCs accounting for 92 % of the total variance of the data, no significant information was obtained since there was no differentiation of the samples related to this class of compounds.

4. Conclusions

In this study, the full validation of a method using GC × GC-ToFMS was performed for the first time, targeting 55 NSO-HETs, demonstrating efficiency in their simultaneous quantification. The analytical method presented a wide range of linearity, low LOD and LOQ values and adequate precision. The trueness was considered suitable given the complexity of the fuel samples.

The fractionation of fuel samples by HPLC led to the removal of matrix interferents and the enrichment of the aromatic fraction in NSO-HET, which facilitated the identification and quantification of target analytes compared to unfractionated fuel samples, especially for the PASH class. The HPLC conditions used were not efficient for carbazoles and benzocarbazoles, highlighting the necessity of future studies to optimize this step for their elution, by testing alternative stationary phases such as C_{18} reverse-phase columns that can help to improve the recoveries of these PANHs.

The optimized and validated GC × GC-ToFMS method was applied to fuel samples for NSO-HET analysis. In total, thirty-two NSO-HET belonging to different classes were quantified in these samples. For PASH, the fractionated marine diesel and S-500 presented the highest concentrations of 2,5,7-TMBT and 4-EtDBT; meanwhile, in the PANH class, IND concentrations stood out, appearing in all the fuel samples at a wide range of levels. DBF was the PAOH found with the highest concentrations, especially for the fractionated diesel S-500 sample.

The analytical method demonstrated the capabilities of GC × GC-ToFMS to quantify heteroatom-containing compounds in fuels with limited sample preparation. Finally, considering the broad use of GC × GC-ToFMS in the fuel industry, the proposed method can be readily applied to other fuel types (e.g., jet fuel, biodiesel blends) and shows potential for implementation in routine analytical workflows in this sector.

CRediT authorship contribution statement

Pedro Victor Bomfim Bahia: Writing – review & editing, Writing – original draft, Methodology, Investigation, Formal analysis. **Anaïs Rodrigues:** Writing – review & editing, Formal analysis. **Aleksandra Gorska:** Writing – review & editing, Methodology, Formal analysis. **Paula Albendea:** Writing – review & editing, Formal analysis. **Djulia Bensaada:** Writing – review & editing, Formal analysis. **Pierre-Hugues Stefanuto:** Writing – review & editing, Methodology, Formal analysis. **Jean-François Focant:** Writing – review & editing, Methodology, Formal analysis. **Giorgia Purcaro:** Writing – review & editing, Supervision, Funding acquisition, Conceptualization. **Maria Elisabete Machado:** Writing – review & editing, Supervision, Investigation, Funding acquisition, Conceptualization.

Declaration of competing interest

The authors declare that they have no known competing financial interests or personal relationships that could have appeared to influence the work reported in this paper.

Acknowledgements

The authors acknowledge financial support from the Brazilian agencies: Conselho Nacional de Desenvolvimento Científico e Tecnológico (CNPq, process 140518/2022–3) and Coordenacão de Aperfeicoamento de Pessoal de Nível Superior (CAPES) - Programa Institucional de Internacionalização CAPES PRINT for Ph.D. grant (process 88887.932212/2024–00). Author Anaïs Rodrigues was supported by the University of Liège under Special Funds for Research, IPD-STEMA Program. Authors Aleksandra Gorska, Paula Albandea, and Giorgia Purcaro thank LECO and Restek for their continuous support.

Appendix A. Supplementary data

Supplementary data to this article can be found online at https://doi.org/10.1016/j.aca.2025.344621.

Data availability

Data will be made available on request.

References

[1] R. Gieleciak, D. Hager, N.E. Heshka, Application of a quantitative structure retention relationship approach for the prediction of the two-dimensional gas chromatography retention times of polycyclic aromatic sulfur heterocycle compounds, J. Chromatogr., A 1437 (2016) 191–202, https://doi.org/10.1016/j.chroma.2016.02.006.

[2] M.E. Machado, M.M. Nascimento, P.V.B. Bahia, S.T. Martinez, J. Bittencourt de Andrade, Analytical advances and challenges for the determination of heterocyclic aromatic compounds (NSO-HET) in sediment: a review, TrAC, Trends Anal. Chem. 150 (2022) 116586, https://doi.org/10.1016/j.trac.2022.116586.

[3] F. Cappelli Fontanive, É.A. Souza-Silva, J. Macedo da Silva, E. Bastos Caramão, C. Alcaraz Zini, Characterization of sulfur and nitrogen compounds in Brazilian petroleum derivatives using ionic liquid capillary columns in comprehensive two-dimensional gas chromatography with time-of-flight mass spectrometric detection, J. Chromatogr., A 1461 (2016) 131–143, https://doi.org/10.1016/j.chroma.2016.07.025.

[4] F.A. Franchina, M.E. Machado, P.Q. Tranchida, C.A. Zini, E.B. Caramão, L. Mondello, Determination of aromatic sulphur compounds in heavy gas oil by using (low-)flow modulated comprehensive two-dimensional gas chromatography-triple quadrupole mass spectrometry, J. Chromatogr., A 1387 (2015) 86–94, https://doi.org/10.1016/j.chroma.2015.01.082.

[5] M. Romanczyk, R.D. Deese, T.N. Loegel, A.E. Metz, R.E. Morris, R.A. Kamin, A. M. McDaniel, M.E. Peretich, Examination of two-dimensional gas chromatography with a nitrogen chemiluminescence detector to facilitate quantitation and characterization of nitrogen-containing compounds in petroleum-derived fuels, Energy Fuels 35 (2021) 5867–5878, https://doi.org/10.1021/acs.energyfuels.0c04316.

[6] G.C. Laredo, N.V. Likhanova, I.V. Lijanova, B. Rodriguez-Heredia, J.J. Castillo, P. Perez-Romo, Synthesis of ionic liquids and their use for extracting nitrogen compounds from gas oil feeds towards diesel fuel production, Fuel Process. Technol. 130 (2015) 38–45, https://doi.org/10.1016/j.fuproc.2014.08.025.

[7] M. Li, G.S. Ellis, Qualitative and quantitative analysis of Dibenzofuran, alkyldibenzofurans, and benzo[b]naphthofurans in crude oils and source rock extracts, Energy Fuels 29 (2015) 1421–1430, https://doi.org/10.1021/ef502558a.

[8] S. Kheirollahi, M. BinDahbag, H. Bagherzadeh, Z. Abbasi, H. Hassanzadeh, Improved determination of saturate, aromatic, resin, and asphaltene (SARA) fractions using automated high-performance liquid chromatography approach, Fuel 371 (2024) 131884, https://doi.org/10.1016/j.fuel.2024.131884.

[9] L. Carvalho Dias, P.V.B. Bahia, D. Nery do Amaral, M.E. Machado, Nitrogen compounds as molecular markers: an overview of analytical methodologies for its determination in crude oils and source rock extracts, Microchem. J. 157 (2020) 105039, https://doi.org/10.1016/j.microc.2020.105039.

[10] L.M.L. de Oliveira, D.N. do Amaral, K.L. de A. Ferreira, C.S. Souza, G.M. Hadlich, M.E. Machado, Polycyclic aromatic sulfur heterocycles used as molecular markers in crude oils and source rocks, Org. Geochem. 178 (2023) 104571, https://doi.org/10.1016/j.orggeochem.2023.104571.

[11] B. Yang, W. Hou, K. Zhang, X. Wang, Application of solid-phase microextraction to the determination of polycyclic aromatic sulfur heterocycles in Bohai Sea crude oils, J. Sep. Sci. 36 (2013) 2646–2655, https://doi.org/10.1002/jssc.201300184.

[12] G. Zhang, C. Yang, M. Serhan, G. Koivu, Z. Yang, B. Hollebone, P. Lambert, C. E. Brown, Characterization of nitrogen-containing polycyclic aromatic heterocycles in crude oils and refined petroleum products, in: first ed.Advances in Marine Biology, vol. 81, 2018, pp. 59–96, https://doi.org/10.1016/bs.amb.2018.09.006.

[13] M.E. Machado, E.W. De Menezes, L.P. Bregles, E.B. Caramão, E.V. Benvenutti, C. A. Zini, Palladium(II) chemically bonded to silica surface applied to the separation and identification of polycyclic aromatic sulfur heterocycles in heavy oil, J. Sep. Sci. 36 (2013) 1636–1643, https://doi.org/10.1002/jssc.201200773.

[14] M.E. Machado, L.P. Bregles, E.W. de Menezes, E.B. Caramão, E.V. Benvenutti, C. A. Zini, Comparison between pre-fractionation and fractionation process of heavy gas oil for determination of sulfur compounds using comprehensive two-dimensional gas chromatography, J. Chromatogr., A 1274 (2013) 165–172, https://doi.org/10.1016/j.chroma.2012.12.002.

[15] T. Dutriez, J. Borras, M. Courtiade, D. Thiébaut, H. Dulot, F. Bertoncini, M. C. Hennion, Challenge in the speciation of nitrogen-containing compounds in heavy petroleum fractions by high temperature comprehensive two-dimensional

gas chromatography, J. Chromatogr., A 1218 (2011) 3190–3199, https://doi.org/10.1016/j.chroma.2010.10.056.
[16] D.W. Later, M.L. Lee, K.D. Bartle, R.C. Kong, D.L. Vassilaros, Chemical class separation and characterization of organic compounds in synthetic fuels, Anal. Chem. 53 (1981) 1612–1620, https://doi.org/10.1021/ac00234a017.
[17] J.J. Adams, J.F. Rovani, J.P. Planche, J. Loveridge, A. Literati, I. Shishkova, G. Palichev, I. Kolev, K. Atanassov, S. Nenov, S. Ribagin, D. Stratiev, D. Yordanov, J. Huo, SAR-AD method to characterize eight SARA fractions in various vacuum residues and follow their transformations occurring during hydrocracking and pyrolysis, Processes 11 (2023) 1220, https://doi.org/10.3390/pr11041220.
[18] M. Biedermann, K. Grob, On-line coupled high performance liquid chromatography-gas chromatography for the analysis of contamination by mineral oil. Part 1: method of analysis, J. Chromatogr., A 1255 (2012) 56–75, https://doi.org/10.1016/j.chroma.2012.05.095.
[19] M. Biedermann, K. Grob, Comprehensive two-dimensional GC after HPLC preseparation for the characterization of aromatic hydrocarbons of mineral oil origin in contaminated sunflower oil, J. Sep. Sci. 32 (2009) 3726–3737, https://doi.org/10.1002/jssc.200900366.
[20] N.E. Oro, C.A. Lucy, Analysis of the nitrogen content of distillate cut gas oils and treated heavy gas oils using normal phase HPLC, fraction collection and petroleomic FT-ICR MS data, Energy Fuels 27 (2013) 35–45, https://doi.org/10.1021/ef301116j.
[21] D. Mao, H. Van De Weghe, L. Diels, N. De Brucker, R. Lookman, G. Vanermen, High-performance liquid chromatography fractionation using a silver-modified column followed by two-dimensional comprehensive gas chromatography for detailed group-type characterization of oils and oil pollution, J. Chromatogr., A 1179 (2008) 33–40, https://doi.org/10.1016/j.chroma.2007.09.085.
[22] I.C. Lee, H.C. Ubanyionwu, Determination of sulfur contaminants in military jet fuels, Fuel 87 (2008) 312–318, https://doi.org/10.1016/j.fuel.2007.05.010.
[23] S. Pan, Y. Zhang, J. Bai, Z. Wang, D. Cui, Q. Wang, Investigation of generation mechanisms in nitrogenous compounds of shale oil using GC-NCD and theoretical calculations, J. Energy Inst. 118 (2025) 101950, https://doi.org/10.1016/j.joei.2024.101950.
[24] J.O. Lalah, P.N. Kaigwara, Polynuclear aromatic compounds in kerosene, diesel and unmodified sunflower oil and in respective engine exhaust particulate emissions, Toxicol. Environ. Chem. 87 (2005) 463–479, https://doi.org/10.1080/02772240500316702.
[25] P.Q. Tranchida, M. Maimone, G. Purcaro, P. Dugo, L. Mondello, The penetration of green sample-preparation techniques in comprehensive two-dimensional gas chromatography, TrAC, Trends Anal. Chem. 71 (2015) 74–84, https://doi.org/10.1016/j.trac.2015.03.011.
[26] M. Adahchour, J. Beens, R.J.J. Vreuls, U.A.T. Brinkman, Recent developments in comprehensive two-dimensional gas chromatography (GC × GC). I. Introduction and instrumental set-up, TrAC, Trends Anal. Chem. 25 (2006) 438–454, https://doi.org/10.1016/j.trac.2006.03.002.
[27] R.K. Nelson, C. Aeppli, J. Samuel, H. Chen, A.H.B. De Oliveira, C. Eiserbeck, G. S. Frysinger, R.B. Gaines, K. Grice, J. Gros, G.J. Hall, H.H.F. Koolen, K.L. Lemkau, A.M. McKenna, C.M. Reddy, R.P. Rodgers, R.F. Swarthout, D.L. Valentine, H. K. White, Applications of comprehensive two-dimensional Gas Chromatography (GC × GC) in studying the source, transport, and fate of petroleum hydrocarbons in the environment. Standard Handbook Oil Spill Environmental Forensics, second ed., 2016, pp. 399–448, https://doi.org/10.1016/B978-0-12-809659-8.00008-5.
[28] T.R. Bjerk, E.W. de Menezes, M.B. Pereira, E.B. Caramão, E.V. Benvenutti, C. A. Zini, Silver bonded to silica gel applied to the separation of polycyclic aromatic sulfur heterocycles in heavy gas oil, J. Chromatogr., A 1470 (2016) 104–110, https://doi.org/10.1016/j.chroma.2016.09.064.
[29] I. Aloisi, M. Zoccali, P.Q. Tranchida, L. Mondello, Analysis of organic sulphur compounds in coal tar by using comprehensive two-dimensional gas chromatography-high resolution time-of-flight mass spectrometry, Separations 7 (2020) 3–11, https://doi.org/10.3390/separations7020026.
[30] J.M. da Silva, M.E. Machado, G.P.S. Maciel, D. Dal Molin, E.B. Caramão, Speciation of nitrogen-containing compounds in an unfractionated coal tar sample by comprehensive two-dimensional gas chromatography coupled to time-of-flight mass spectrometry, J. Chromatogr., A 1373 (2014) 159–168, https://doi.org/10.1016/j.chroma.2014.11.004.
[31] C. Von Mühlen, E.C. De Oliveira, C.A. Zini, E.B. Caramão, P.J. Marriott, Characterization of nitrogen-containing compounds in heavy gas oil petroleum fractions using comprehensive two-dimensional gas chromatography coupled to time-of-flight mass spectrometry, Energy Fuels 24 (2010) 3572–3580, https://doi.org/10.1021/ef1002364.
[32] M.E. Machado, F. Cappelli Fontanive, J.V. De Oliveira, E.B. Caramão, C. Alcaraz Zini, Identification of organic sulfur compounds in coal bitumen obtained by different extraction techniques using comprehensive two-dimensional gas chromatography coupled to time-of-flight mass spectrometric detection, Anal. Bioanal. Chem. 401 (2011) 2433–2444, https://doi.org/10.1007/s00216-011-5171-4.
[33] M.E. Machado, E.B. Caramão, C.A. Zini, Investigation of sulphur compounds in coal tar using monodimensional and comprehensive two-dimensional gas chromatography, J. Chromatogr., A 1218 (2011) 3200–3207, https://doi.org/10.1016/j.chroma.2010.11.077.
[34] ANP, Agência Nacional de Petróleo, Gás Natural e Biocombustíveis, Resolução ANP N° 968, 30 de abril de 2024 - DOU de 02-05-2024. https://atosoficiais.com.br/anp/resolucao-n-968-2024/, 2024. (Accessed 3 September 2025).
[35] G. Bauwens, S. Pantó, G. Purcaro, Mineral oil saturated and aromatic hydrocarbons quantification: Mono- and two-dimensional approaches, J. Chromatogr., A 1643 (2021) 462044, https://doi.org/10.1016/j.chroma.2021.462044.
[36] G. Bauwens, C. Conchione, N. Sdrigotti, S. Moret, G. Purcaro, Quantification and characterization of mineral oil in fish feed by liquid chromatography-gas chromatography-flame ionization detector and liquid chromatography-comprehensive multidimensional gas chromatography-time-of-flight mass spectrometer/flame ioniza, J. Chromatogr., A 1677 (2022) 463208, https://doi.org/10.1016/j.chroma.2022.463208.
[37] I. Idowu, W. Johnson, O. Francisco, T. Obal, C. Marvin, P.J. Thomas, C.D. Sandau, J. Stetefeld, G.T. Tomy, Comprehensive two-dimensional gas chromatography high-resolution mass spectrometry for the analysis of substituted and unsubstituted polycyclic aromatic compounds in environmental samples, J. Chromatogr., A 1579 (2018) 106–114, https://doi.org/10.1016/j.chroma.2018.10.030.
[38] D. Huang, L. Gao, M. Zheng, L. Qiao, C. Xu, K. Wang, S. Wang, Screening organic contaminants in soil by two-dimensional gas chromatography high-resolution time-of-flight mass spectrometry: a non-target analysis strategy and contaminated area case study, Environ. Res. 205 (2022) 112420, https://doi.org/10.1016/j.envres.2021.112420.
[39] A. Mostafa, M. Edwards, T. Górecki, Optimization aspects of comprehensive two-dimensional gas chromatography, J. Chromatogr., A 1255 (2012) 38–55, https://doi.org/10.1016/j.chroma.2012.02.064.
[40] T. Dijkmans, K.M. Van Geem, M.R. Djokic, G.B. Marin, Combined comprehensive two-dimensional gas chromatography analysis of polyaromatic hydrocarbons/polyaromatic sulfur-containing hydrocarbons (PAH/PASH) in complex matrices, Ind. Eng. Chem. Res. 53 (2014) 15436–15446, https://doi.org/10.1021/ie5000888.
[41] M. Thompson, S.L.R. Ellison, R. Wood, Harmonized guidelines for single-laboratory validation of methods of analysis (IUPAC Technical report), Pure Appl. Chem. 74 (2002) 835–855, https://doi.org/10.1351/pac200274050835.
[42] R.D. Ledesma, P. Valero-Mora, G. Macbeth, The scree test and the number of factors: a dynamic graphics approach, Spanish J. Psychol. 18 (2015) E11, https://doi.org/10.1017/sjp.2015.13.
[43] M. Li, X. Liu, T.G. Wang, W. Jiang, R. Fang, L. Yang, Y. Tang, Fractionation of dibenzofurans during subsurface petroleum migration: based on molecular dynamics simulation and reservoir geochemistry, Org. Geochem. 115 (2018) 220–232, https://doi.org/10.1016/j.orggeochem.2017.10.006.
[44] R. Becker, U. Dorgerloh, M. Helmis, J. Mumme, M. Diakité, I. Nehls, Hydrothermally carbonized plant materials: patterns of volatile organic compounds detected by gas chromatography, Bioresour. Technol. 130 (2013) 621–628, https://doi.org/10.1016/j.biortech.2012.12.102.
[45] C. Manzano, E. Hoh, S.L.M. Simonich, Improved separation of complex polycyclic aromatic hydrocarbon mixtures using novel column combinations in GC × GC/ToF-MS, Environ. Sci. Technol. 46 (2012) 7677–7684, https://doi.org/10.1021/es301790h.
[46] H.E. Toraman, K. Franz, F. Ronsse, K.M. Van Geem, G.B. Marin, Quantitative analysis of nitrogen containing compounds in microalgae based bio-oils using comprehensive two-dimensional gas-chromatography coupled to nitrogen chemiluminescence detector and time of flight mass spectrometer, J. Chromatogr., A 1460 (2016) 135–146, https://doi.org/10.1016/j.chroma.2016.07.009.
[47] H. Engelhardt, C. Blay, J. Saar, Reversed phase chromatography - the mystery of surface silanols, Chromatographia 62 (2005) 19–29, https://doi.org/10.1365/s10337-005-0573-0.
[48] E.B. Frolov, Liquid chromatography of petroleum carbazoles, Org. Geochem. 26 (1997) 43–47, https://doi.org/10.1016/S0146-6380(96)00151-9.
[49] M. Li, S.R. Larter, D. Stoddart, M. Bjorøy, M. Bjorøy, Liquid chromatographic separation schemes for pyrrole and pyridine nitrogen aromatic heterocycle fractions from crude oils suitable for rapid characterization of geochemical samples, Anal. Chem. 64 (1992) 1337–1344, https://doi.org/10.1021/ac00037a007.
[50] H. Carlsson, C. Östman, Clean-up and analysis of carbazole and acridine type polycyclic aromatic nitrogen heterocyclics in complex sample matrices, J. Chromatogr., A 790 (1997) 73–82, https://doi.org/10.1016/S0021-9673(97)00759-0.
[51] F.C.Y. Wang, W.K. Robbins, M.A. Greaney, Speciation of nitrogen-containing compounds in diesel fuel by comprehensive two-dimensional gas chromatography, J. Sep. Sci. 27 (2004) 468–472, https://doi.org/10.1002/jssc.200301643.
[52] S.D. Sumbogo Murti, K. Sakanishi, O. Okuma, Y. Korai, I. Mochida, Detailed characterization of heteroatom-containing molecules in light distillates derived from tanito harum coal and its hydrotreated oil, Fuel 81 (2002) 2241–2248, https://doi.org/10.1016/S0016-2361(02)00159-X.
[53] S. Hashimoto, T. Yoshikatsu, F. Akihiro, I. Hiroyasu, T. Kiyoshi, S. Yasuyuki, U. Masa-aki, K. Akihiko, T. Kazuo, O. Hideyuki, A. Katsunori, Quantification of polychlorinated dibenzo-p-dioxins and dibenzofurans by direct injection of sample extract into the comprehensive multidimensional gas chromatograph/high-resolution time-of-flight mass spectrometer, J. Chromatogr., A 1178 (2008) 187–198, https://doi.org/10.1016/j.chroma.2007.11.067.
[54] Y. Xu, Y. Zhao, X. Guo, Y. Fang, Characterization of trace oxygenates from Co-processing of bio-oils with petroleum-derived feed with GC × GC-MS, Energy Fuels 36 (2022) 12076–12084, https://doi.org/10.1021/acs.energyfuels.2c02348.
[55] J. García-Bellido, M. Redondo-Velasco, L. Freije-Carrelo, G. Burnens, M. Moldovan, B. Bouyssiere, P. Giusti, J.R. Encinar, Sensitive detection and quantification of oxygenated compounds in complex samples using GC-combustion-MS, Anal. Chem. 96 (2024) 10756–10764, https://doi.org/10.1021/acs.analchem.4c01858.
[56] F. Correddu, A. Cesarani, C. Dimauro, G. Gaspa, N.P.P. Macciotta, Principal component and multivariate factor analysis of detailed sheep milk fatty acid profile, J. Dairy Sci. 104 (2021) 5079–5094, https://doi.org/10.3168/jds.2020-19087.

[57] M. Li, T.G. Wang, B.R.T. Simoneit, S. Shi, L. Zhang, F. Yang, Qualitative and quantitative analysis of dibenzothiophene, its methylated homologues, and benzonaphthothiophenes in crude oils, coal, and sediment extracts, J. Chromatogr., A 1233 (2012) 126–136, https://doi.org/10.1016/j.chroma.2012.01.086.

[58] J.L. Rivera, P. Navarro-Santos, L. Hernandez-Gonzalez, R. Guerra-Gonzalez, Reactivity of alkyldibenzothiophenes using theoretical descriptors, J. Chem. 2014 (2014), https://doi.org/10.1155/2014/215074.

[59] G.P.S. Maciel, M.E. Machado, M.E. Da Cunha, E. Lazzari, J.M. Da Silva, R. A. Jacques, L.C. Krause, J.A.S. Barros, E.B. Caramão, Quantification of nitrogen compounds in diesel fuel samples by comprehensive two-dimensional gas chromatography coupled with quadrupole mass spectrometry, J. Sep. Sci. 38 (2015) 4071–4077, https://doi.org/10.1002/jssc.201500011.